SEMARAK ILMU PUBLISHING

Journal of Advanced Research in Fluid Mechanics and Thermal Sciences

Journal homepage:
https://semarakilmu.com.my/journals/index.php/fluid_mechanics_thermal_sciences/index
ISSN: 2289-7879

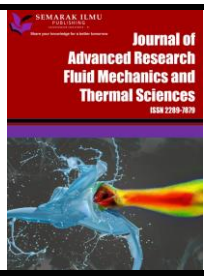

Investigation on the Blade Number of Pico-scale Crossflow Turbine for Low Head by Numerical Method

Dendy Adanta[1], Ilham Saputra[1], Dewi Puspita Sari[2], Imam Syofii[2], Ismail Thamrin[1,*], Irsyadi Yani[1], Anthony Costa[3], Akbar Teguh Prakoso[1], Ahmad Fudholi[4,5], Wadirin[2]

[1] Department of Mechanical Engineering, Faculty of Engineering, Universitas Sriwijaya, Ogan Ilir – 30662, South Sumatera, Indonesia
[2] Study Program of Mechanical Engineering Education, Faculty of Teacher Training and Education, Universitas Sriwijaya, Ogan Ilir – 30662, South Sumatera, Indonesia
[3] Department of Civil Engineering, Faculty of Engineering, Universitas Sriwijaya, Ogan Ilir – 30662, South Sumatera, Indonesia
[4] Research Center for Energy Conversion and Conservation, National Research and Innovation Agency (BRIN), Serpong, 15314, Indonesia
[5] Solar Energy Research Institute, Universiti Kebangsaan Malaysia, 43600 Bangi, Selangor, Malaysia

ARTICLE INFO

Article history:
Received 12 January 2024
Received in revised form 20 May 2024
Accepted 1 June 2024
Available online 30 June 2024

Keywords:
Crossflow turbine; pico hydro; computational fluid dynamic; energy conversion; low head

ABSTRACT

Pico-scale crossflow turbines (CFT) can be an alternative solution to meet electrical energy needs, especially in remote rural areas. CFT is recommended because of its suitability in low head (< 5 m) conditions and fluctuating discharge conditions. One of the parameters that influences the performance of a CFT is the number of blades of the runner. CFT was discovered in 1903 and is still developing; however, the study of the physical phenomena of flow due to the blade number on the energy conversion process has yet to be comprehensively depicted. Therefore, this study aims to analyze the effect of the blade's number of runners on CFT performance using the computational fluid dynamics (CFD) method. The CFD method can visualize the flow field more detail than analytical and experimental. The CFD method is run with a moving mesh feature (transient) and pressure-based solver with a head condition of 3 m. The blades number studied were 16, 18, 22, 24, 26, and 30. Based on the results, the relationship of the CFT efficiency to blade number is described using a second-order multiple regression polynomial, and runner rotation is parabolic. Based on the performance curve, the CFT with 26 blades has the highest performance for low-head conditions.

1. Introduction

In the last few decades, developing countries have realized that micro and pico-scale hydropower is important in economic development in remote areas, especially mountainous areas [1]. Therefore, micro and pico-scale hydropower technology development continues to be carried out to meet energy needs in remote areas [2-9]. Utilizing water energy on a pico scale requires a combination of efficiency, economy, and compactness. Some engineers suggest that CFTs are appropriate turbines for remote areas as pico-scale hydroelectric power systems. CFT has several advantages, namely

* *Corresponding author.*
E-mail address: ismailthamrin@ft.unsri.ac.id

https://doi.org/10.37934/arfmts.118.2.112

simple construction, good performance in various flow variations, operation at low head (< 5 m) conditions, and a relatively more straightforward fabrication process [10-13].

The feasibility of CFT being applied at the pico scale continues to be developed. The CFT research that has been carried out previously is divided into two, namely experimental and numerical-based research. Experimental CFT research was first carried out by Mockmore and Merryfield [14] and succeeded in proposing empirical equations to determine the crossflow turbine runner and nozzle geometry (runner outer diameter and nozzle discharge angle) through head (H), discharge (Q), and specific speed (NS). This was followed by Desai and Aziz [15], who proposed the ratio of the inner diameter (d) and outer diameter (D) of the CFT runner of 0.65.

In a numerical case study, efforts to improve CFT performance were carried out by Acharya *et al.,* [16], who investigated runner speed, flow characteristics, and turbine geometry optimization. Then, Aliman *et al.,* [17] used a 2-D steady-state approach to evaluate nozzle efficiency. They suggested using the CFD method to study the flow field CFT because it is more efficient than analytics and experiments.

From numerical and experimental studies, angle of attack (α) and blade angle (β_1 for inlet and β_2 for outlet) are important geometries in improving performance. It is noted that three studies discuss in detail the geometry of CFT blades for low head (< 5 m) conditions, as shown in Table 1.

Table 1
Summary of CFT feasibility researchers for low-head

Authors	α_1	β_1	β_2	z	η
De Andre *et al.,* [18]	16	120	90	24	71%
Sammartano *et al.,* [12,19], Sinagra *et al.,* [20,21]	22	38.9	90	35	85.6%
Adhikari and Wood [22,23], Adhikari [24]	22	39	90	30	88%

The CFT design uses a velocity triangle approach to determine α_1, β_1, C_1, and U_1 until the momentum change process (due to the impact of water hitting the blade). However, the velocity triangle approach cannot accommodate the number of blades. Achebe *et al.,* [8], and Mockmore and Merryfield [14] proposed a formulation to determine the blade number CFT using a constant *k* between 0.075 to 0.1. However, the optimum *k* for each CFT depends on the design and geometry. Mathematically, the CFT blade number is between 16 and 30 blades. So far, determining the blade number uses experimental methods, considered expensive and time-consuming. Hence, the CFD method is to find the optimum number of blades for the low-head. Therefore, this study aims to investigate the effect of the blade number of pico-scale CFT using the CFD method.

2. Methodology

2.1 Analytical Method

The character of CFT is that the conversion process occurs twice. The CFT design uses velocity triangle analysis, so that approach is applied at both stages. Figure 1 shows a detailed CFT design algorithm.

The initial boundary conditions of designing a CFT determine the angle of attack (α_1), outlet blade angle (β_2 and β_4), head (H), and tip speed ratio ($U_1/C_{1,x}$ or ϕ). The inlet absolute velocity (C_1) is a function of H and head loss in the nozzle (*k*), assuming a *k* of 5% (0.95). Therefore, C_1 becomes:

$$C_1 = k\sqrt{2 \cdot g \cdot \mathrm{H}} \tag{1}$$

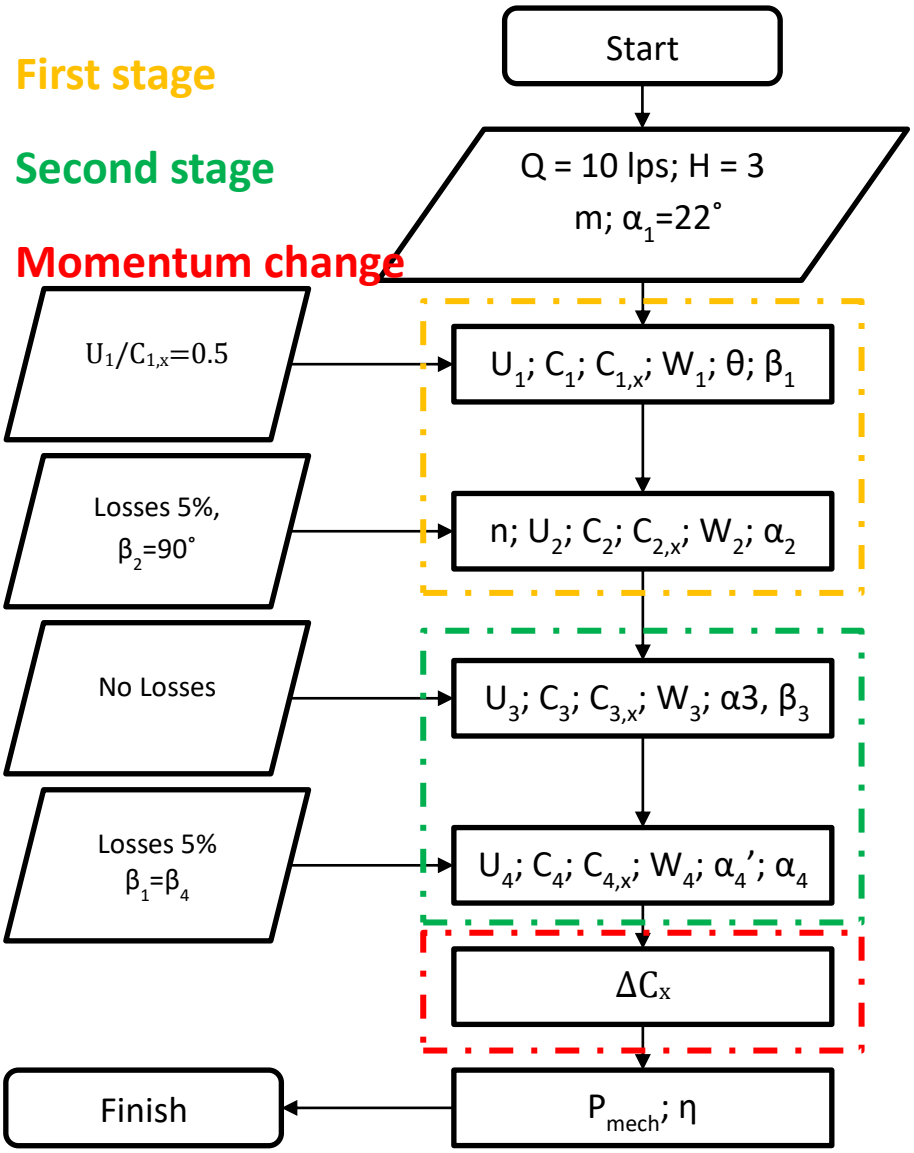

Fig. 1. Flowchart designing CFT

Then, convert C_1 to tangential axis ($C_{1,x}$) using

$$C_{1,x} = C_1 \cdot \cos \alpha_1 \tag{2}$$

The following equation is fulfilled to get the maximum efficiency of CFT

$$2 \cdot \tan \alpha_1 = \tan \beta_1 \tag{3}$$

β_1 is the inlet blade angle formed by the relative velocity (W_1) to the tangential velocity of the runner (U_1). After U_1 determine, then calculate the runner diameter (D)

$$U = \omega \cdot 0.5D \tag{4}$$

0.5D is runner radius (r). ω is used to calculate runner rotation (n). It is assumed that there is an energy loss of 5% due to water rubbing against the blade walls so that W_2=0.95·W_1. Further, U_2 is a function of n. Therefore, the C_2 can be predicted using the Phytagorean theorem, and $C_{2,x}$ analyzed

using trigonometry concepts where the function of β_2 and C_2. In the second stage, there are no losses from the first stage to the second stage, so the component of 3 is similar to 2. Therefore, $\beta_1 = \beta_4$, $U_1 = U_4$, and $W_4 = 0.95 \cdot W_3$.

After analyzing the energy conversion using the velocity triangle approach, the next is to determine the geometry of the CFT runner. The following is an equation for calculating the radius of the blade (r_{blade}) and the angle of blade curvature (δ).

$$r_{blade} = \frac{R^2 - r^2}{2R \cdot \cos \beta_1} b \tag{5}$$

$$\tan \frac{\delta}{2} = \frac{\cos \beta_1}{r/_{R + \sin \beta_1}} \tag{6}$$

Then, the blade number (z) is calculated based on the empirical equation proposed by Achebe *et al.,* [8], and Mockmore and Marryfield [14]

$$z = \frac{\pi \cdot D}{s}; s = \frac{j \cdot D}{\sin \beta_1}; j = 0.075 - 0.1 \tag{7}$$

Figure 2 shows the CFT design results. Based on Figure 2, the outer runner diameter (D) of 100 mm, inner runner diameter (d) of 65 mm, nozzle height (S_0) of 30.6 mm, nozzle width (B) of 60 mm, turbine width (w) of 60 mm, $_{blade}$ radius of 18.56 mm, α_1 of 22°, β_1 of 40°, β_2 of 90°, and inlet discharge angle (λ) of 90° [14,17,25]. The z based on calculation using Eq. (5) is 16, 18, 22, 24, 26, and 30 blades; it is similar to previous study uses 18, 20, 25, and 35 [12,20,22,25-27].

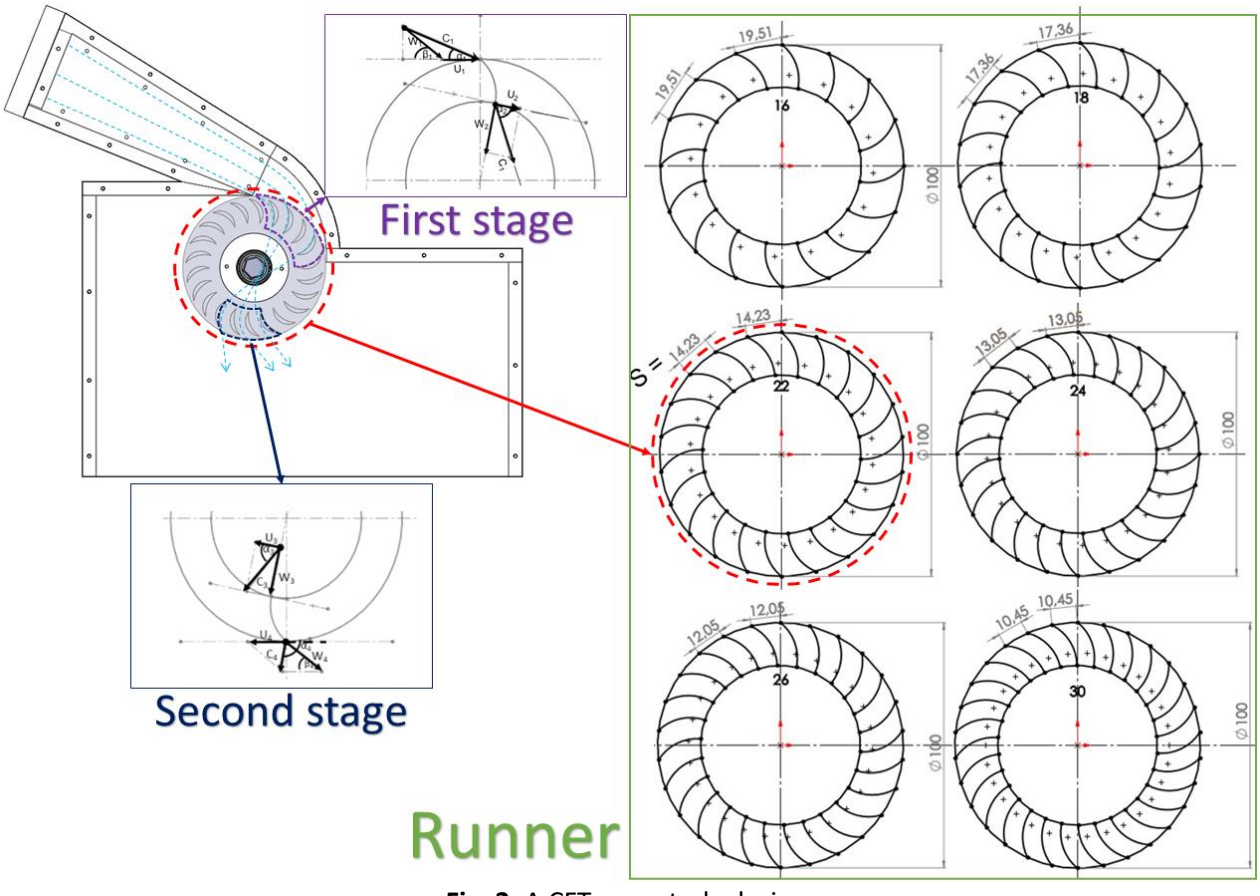

Fig. 2. A CFT case study design

2.2 Numerical Method

The simulation is run using commercial CFD software where continuity equations are employed

$$\frac{\partial \rho}{\partial t} + \frac{\partial \rho u}{\partial x} + \frac{\partial \rho v}{\partial y} = 0 \tag{8}$$

Then, Reynolds-averaged Navier-Stokes (RANS) is run as a numerical calculation of momentum

$$\frac{\partial \rho uv}{\partial t} + \frac{\partial \rho uv}{\partial y} = -\frac{\partial p}{\partial x} + \frac{\partial \tau_{xy} - \rho u'v'}{\partial y} + \rho g_x \tag{9}$$

-ρu'v' is Reynolds stress

$$-\rho u'v' = \mu_t \left[\frac{\partial u}{\partial y} + \frac{\partial v}{\partial x}\right] - \frac{2}{3}\left[\rho k + \mu_t \frac{\partial u}{\partial y}\right]\delta_{xy} \tag{10}$$

Turbulent flow prediction uses a 2-equation turbulent model, namely standard *k-ε*. For *k*

$$\frac{\partial (\rho k)}{\partial t} + \frac{\partial (\rho k u)}{\partial y} = \frac{\partial}{\partial x}\left(\left(\mu + \frac{\mu_t}{\sigma_k}\right)\frac{\partial \rho k}{\partial y}\right) + G_k + G_b + \rho\varepsilon + Y_M + S_k \tag{11}$$

For *ε*:

$$\frac{\partial (\rho \varepsilon)}{\partial t} + \frac{\partial (\rho \varepsilon u)}{\partial y} = \frac{\partial}{\partial x}\left(\left(\mu + \frac{\mu_t}{\sigma_\varepsilon}\right)\frac{\partial \varepsilon}{\partial y}\right) + C_{1\varepsilon}\frac{\varepsilon}{k}(G_k + C_{3\varepsilon}G_b) - C_{2\varepsilon}\rho\frac{\varepsilon^2}{k} + S_\varepsilon \tag{12}$$

$C_{1\varepsilon}$ is Bachelor's constant, and $C_{2\varepsilon}$ is Kolmogorov's constant. The Kolmogorov's constant represents the turbulent spectrum process occurring, and Bachelor's r constant epresents the turbulence and mixing produced by flow fluctuations [28,29]. Figure 3 shows a boundary condition employed for the CFT simulation.

Based on Figure 3, the simulation was run in 2 phase conditions, assuming the water from the inlet is 100% (no air) and the turbine domain is 100% air (initial condition, no water). The prediction of the physical phenomenon of air and water interaction using the volume of fluid (VoF) approach

$$\frac{\partial}{\partial t}(\alpha_n \rho_n) + \frac{\partial}{\partial y}(\alpha_n \rho_n \alpha_n v_n) = \frac{1}{V}\sum_{m=1}^{all-phase} \dot{m}_{mn} - \dot{m}_{nm} \tag{13}$$

The mixture calculation of air and water for density (ρ) and viscosity (μ)

$$\rho = \alpha_w \rho_w + \alpha_a \rho_a; \mu = \alpha_w \mu_w + \alpha_a \mu_a \tag{14}$$

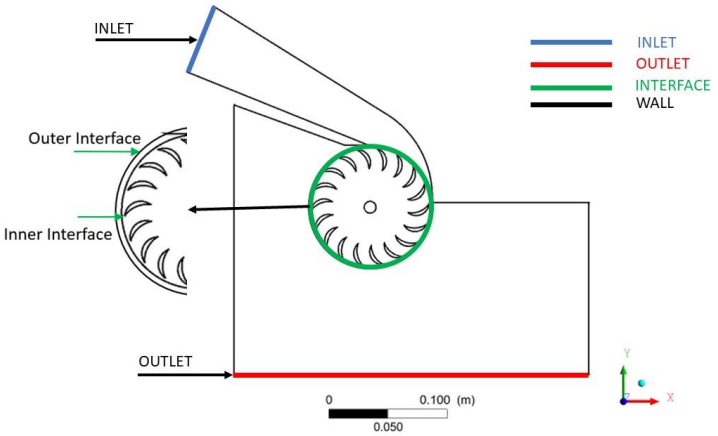

Fig. 3. Boundary conditions

2.3 Mesh Independence Test

The mesh independence test uses three mesh numbers: 249k normalized to 1 (fine), 206k to 1.1 (medium), and 185k to 1.16 (coarse). The grid convergence index (GCI) method is used to determine the optimum mesh numbers; the details of the GCI calculation method refer to Adanta *et al.,* [30]. Based on the simulation, the fine mesh has a force (F) of 70.22 N·m, medium of 66.82 N·m, and coarse of 59.18 N·m. Then, the exact value (F_{exact}) by extrapolation calculation for mesh goes to the continuum of 70.84 N·m. Figure 4 shows a summary of the GCI calculation results. Figure 4 shows the error GCI for mesh fine to medium of 1.094% and for medium to coarse of 7.508%. Therefore, the simulation was run using a 249k mesh number since it has an error below 3%. The visualization of the 249k mesh number can be seen in Figure 4.

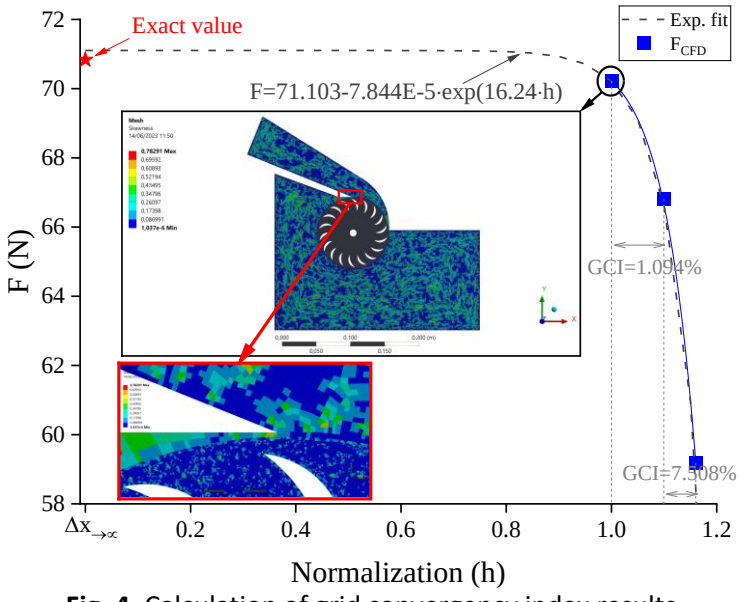

Fig. 4. Calculation of grid convergency index results

3. Results

3.1 Results

Figure 5 depicts the relationship of torque (τ) and mechanical power (P_{mech}) towards n; a is τ towards n, and b is P_{mech} towards n). Based on Figure 5(a), the relationship of τ and n is linear, with

the lowest τ produced by 24-blades of 3.85 N·m at 800 rpm. In contrast, the highest τ of 10.56 N·m is produced by 26-blades at 300 rpm. Then, based on Figure 5(b), the relationship of P_{mech} and n is a parabola curve. The lowest P_{mech} produced by 18-blades is 285.46 W at 300 rpm. Meanwhile, the highest P_{mech} produced 26 blades of 389.69 W at 500 rpm.

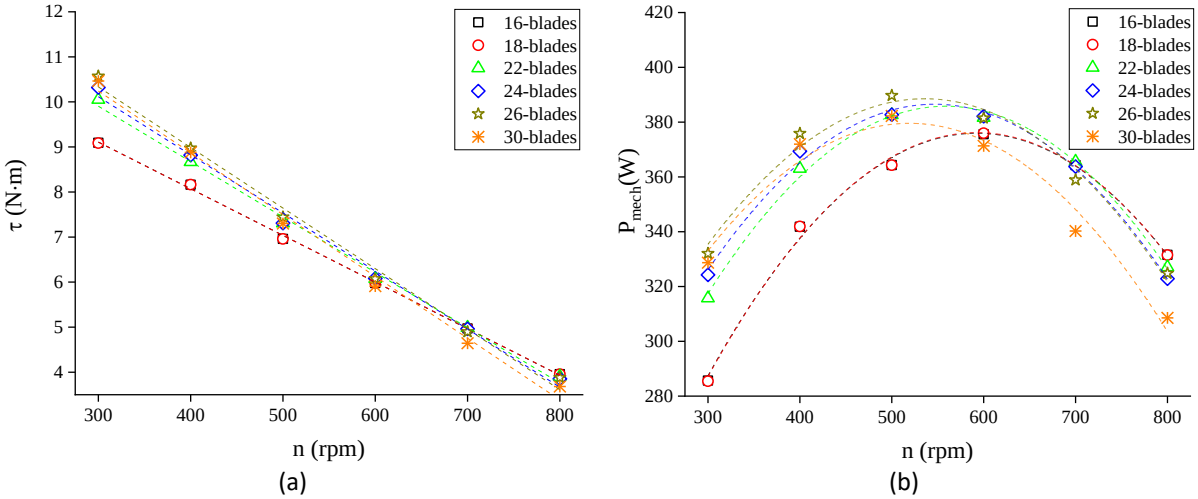

Fig. 5. The relation of τ and P_{mech} toward n: (a) τ toward n; (b) P_{mech} toward n

Figure 6 depicts the relation of η toward n and N_s; a is η toward n, and b is η toward N_s. Based on Figure 6, the relation η toward n and N_s is a parabolic curve. Based on Figure 6(a), the runner of 16-blades, 18-blades, and 30-blades produces lower efficiency than 22-blades of 0.75, 24-blades of 0.76, and 26-blades of 0.76. The 26-blade runner configuration has an efficiency of 0.75 - 0.76 at 500 to 700 rpm- the 26-blades are considered better than the 24-blades, which have an efficiency of 0.76 at 600 – 700 rpm because their operational range is wider than others. Based on Figure 6(b), the N_s range for 26-blades is more profitable than 24-blades. With the N_s of 110 to 120, the efficiency of the 24-blades drastically decreases, unlike other configurations. At 300 to 600 rpm (low rotation) or N_s of 42 to 95, the 26-blade configuration is the best compared to 24-blade, 22-blade, 30-blade, 16-blade, and 18-blades.

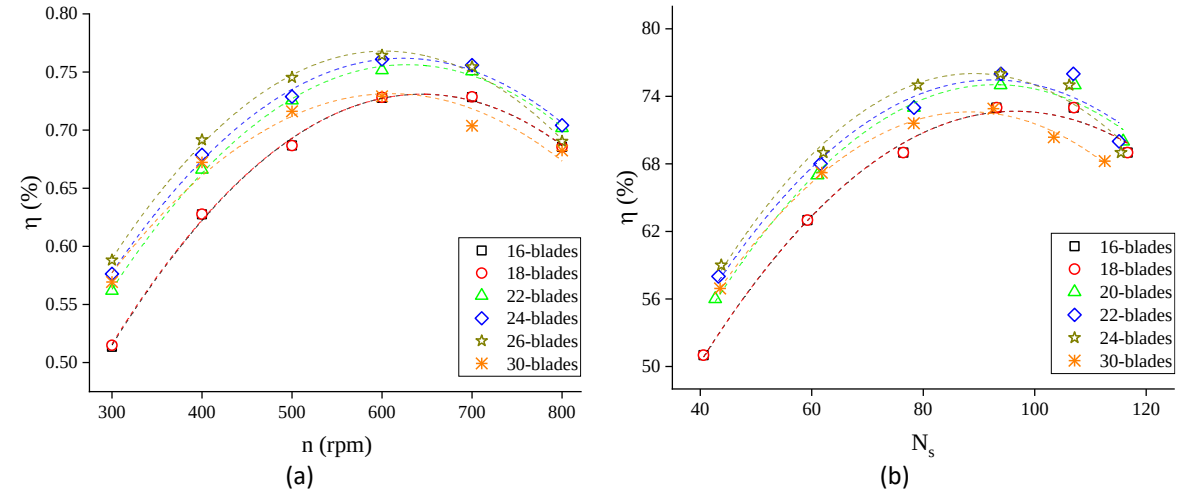

Fig. 6. The relation of η toward n and N_s: (a) η toward n; (b) η toward N_s

3.2 Discussions

Figure 7 shows CFD results for 26-blade, a for streamline velocity, and b for pressure contour. As shown in Figure 7(a), the water velocity increases from the inlet towards the blade, indicating that the water's potential energy at the inlet is slowly being converted into kinetic energy at the nozzle. Figure 7(a) indicates that the designed nozzle works as it should (design nozzle verified). Based on Figure 7(b), the water pressure will decrease along the nozzle, indicating it is moving towards atmospheric (ambient) pressure. Pressure decreases are based on Bernoulli's theorem: pressure is inversely proportional to velocity and vice versa.

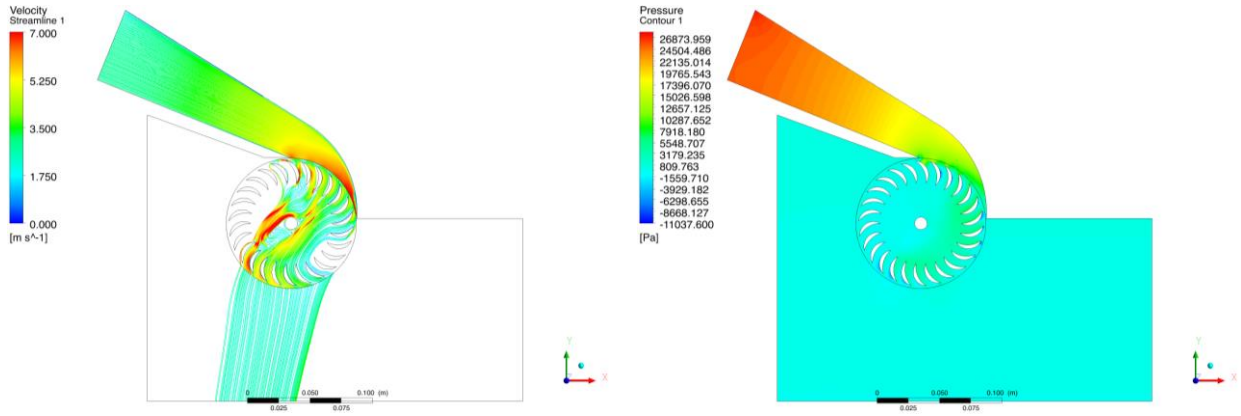

(a) (b)

Fig. 7. Visualization CFT results for 26-blades: (a) Velocity streamline, (b) Pressure contour

Figure 8 depicts the contour of water flowing from the inlet, hitting the turbine blade, and finally leaving the turbine, a for 16-blade and b for 24-blade. Based on Figure 8, runners for configuration of 16-blades have nine active blades, and 24-blades have 13. The active blade number affects the runner in absorbing water energy; the more it is, the better. Therefore, the runner with 24-blades produces greater mechanical power (P_{mech}) compared to the 16-blades, according to the simulation results. However, increasing the blade number further inhibits water flow, so it is only sometimes accompanied by increased CFT performance, which is the maximum point.

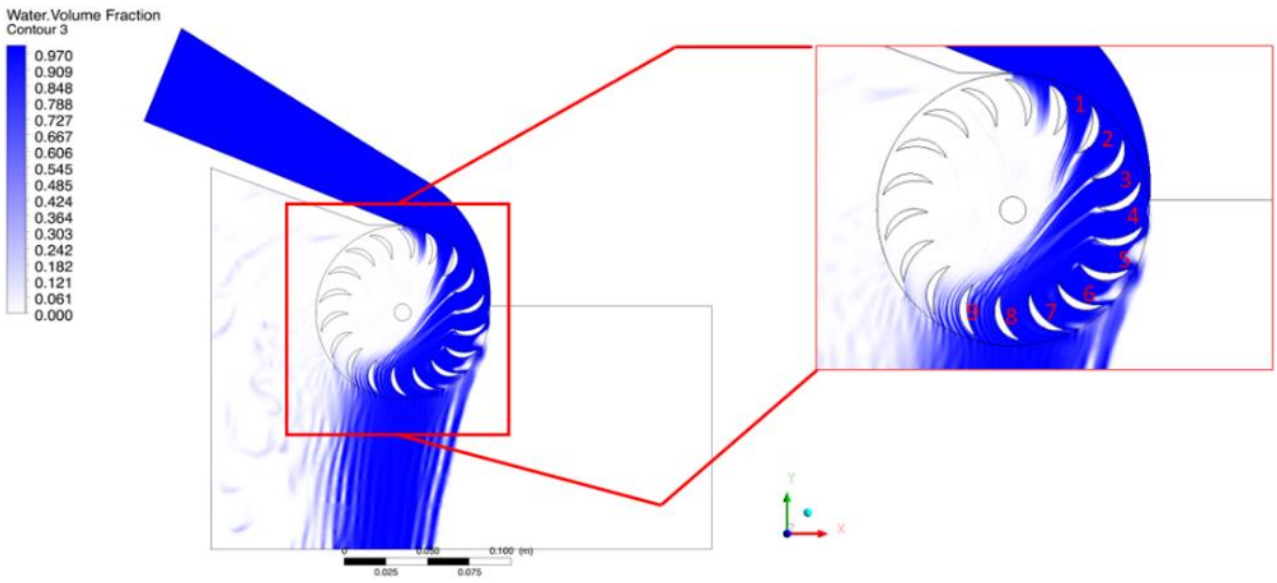

(a)

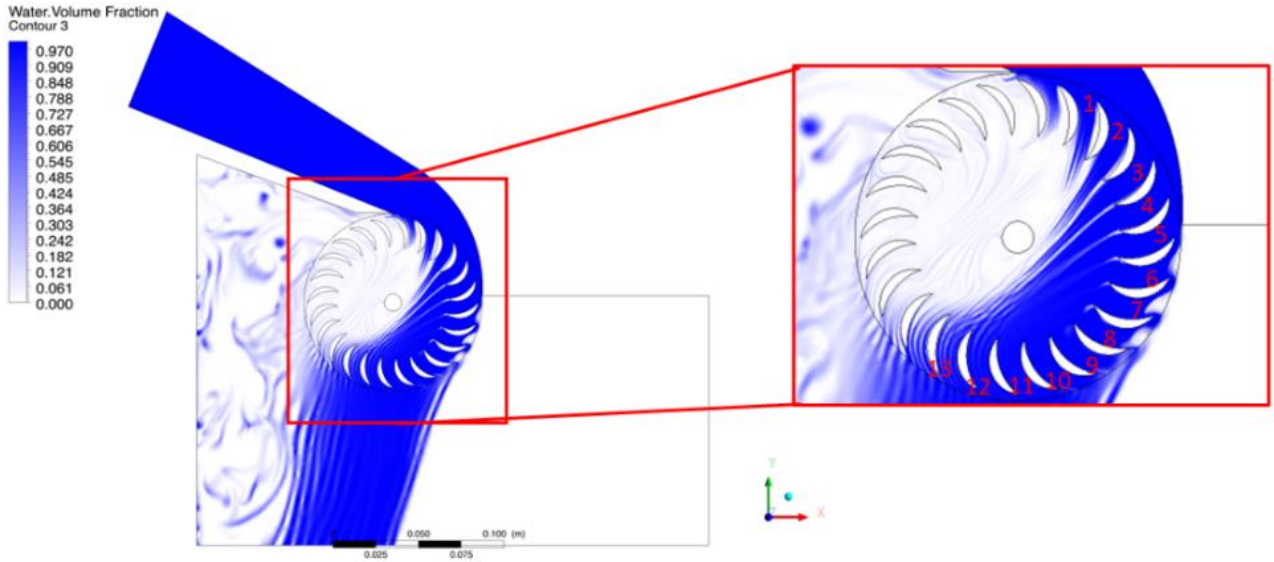

(b)

Fig. 8. Visualization of water volume fraction: (a) 16-blades, (b) 24-blades

Figure 9 depicts the analysis results using multiple polynomial regression order 2 of the efficiency relationship to the number of blades and specific speed. The multiple regression polynomial order 2 allows determining the influence of mechanical power, turbine head, and number of blades on CFT performance.

$$\eta = -35.82 + 3.367 \cdot z + 1.559 \cdot N_s - 0.067 \cdot z^2 - 0.007 \cdot {N_s}^2 - 0.0075 \cdot z \cdot N_s \quad (15)$$

Based on multiple regression polynomial order two calculations, the coefficient of determination (R^2) is 0.977, indicating that around 97.7% of CFT efficiency is influenced by specific speed and blade number. The results of calculating the root mean squared error (RMSE) for Eq. (15) of 1.03%; the prediction result category has good accuracy. Table 2 shows an analysis of variance for the relation of efficiency toward blade number and specific speed CFT for the low head (< 5 m).

Table 2
Analysis of variance results for the relation of efficiency toward blade number and specific speed CFT

	Degrees of freedom	Sum of squares	Mean squares	F	Significance F
Regression	5	1627.244	325.448	238	1.24E-23
Residual	30	38.2519	1.275		
Total	35	1665.49			

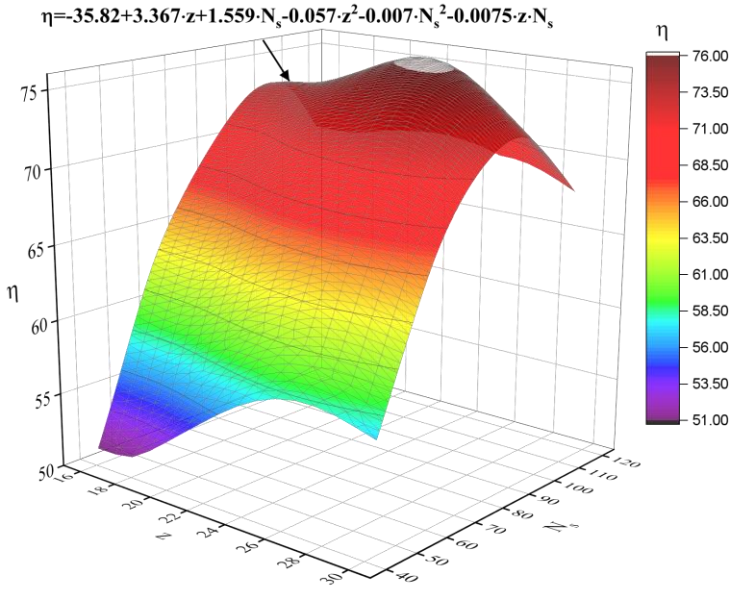

Fig. 9. Relationship of efficiency to blade numbers and specific speed CFT

4. Conclusions and Future Work

This work investigated the effect of the blade's number of pico-scale CFT using the CFD method. The blade number based on calculation is 16, 18, 22, 24, 26, and 30 blades; it is similar to the previous study using 18, 20, 25, and 35 [12,20,22,25-27]. Based on the simulation results, a pico scale CFT with a configuration runner using 26 blades is more profitable than 16, 18, 22, 24, and 30 blades; this is because 26-blade has an efficiency of 0.75 - 0.76 at 500 to 700 rpm; this operational range is wider than other. In addition, for low rotation (300 to 600 rpm), the 26-blade configuration is the best compared to the 24-blade, 22-blade, 30-blade, 16-blade, and 18-blade. As a recommendation, the results of this study necessary validation from experimental data.

Acknowledgements

The research/publication of this article was funded by DIPA of Public Service Agency of Universitas Sriwijaya 2024. SP DIPA number of 023.17.2.677515/2023, on November 24, 2023. In accordance with Rector's Decree Number: 0013/UN9/LP2M.PT/2024, on May 20, 2024.

References

[1] Anand, R. S., C. P. Jawahar, Evangelos Bellos, and Anders Malmquist. "A comprehensive review on Crossflow turbine for hydropower applications." *Ocean Engineering* 240 (2021): 110015. https://doi.org/10.1016/j.oceaneng.2021.110015

[2] Ho-Yan, Bryan. "Design of a low head pico hydro turbine for rural electrification in Cameroon." *PhD diss., University of Guelph*, 2012.

[3] Adhikari, Pradhumna, Umesh Budhathoki, Shiva Raj Timilsina, Saurav Manandhar, and Tri Ratna Bajracharya. "A study on developing pico propeller turbine for low head micro hydropower plants in Nepal." *Journal of the Institute of Engineering* 9, no. 1 (2014): 36-53. https://doi.org/10.3126/jie.v9i1.10669

[4] Vicente, Silvia, and Hans Bludszuweit. "Flexible design of a pico-hydropower system for Laos communities." *Renewable Energy* 44 (2012): 406-413. https://doi.org/10.1016/j.renene.2012.02.011

[5] Gladstone, Scott, Victoria Tersigni, Kevin Francfort, and Julie Ann Haldeman. "Implementing pico-hydropower sites in rural Rwanda." *Procedia Engineering* 78 (2014): 279-286. https://doi.org/10.1016/j.proeng.2014.07.068

[6] Thomas, Brian. "Pico-hydropower franchising in rural Honduras." *International Journal for Service Learning in Engineering, Humanitarian Engineering and Social Entrepreneurship* 6, no. 1 (2011): 46-63.

https://doi.org/10.24908/ijsle.v6i1.3213
[7] Williams, A. A., and R. Simpson. "Pico hydro-Reducing technical risks for rural electrification." *Renewable Energy* 34, no. 8 (2009): 1986-1991. https://doi.org/10.1016/j.renene.2008.12.011
[8] Achebe, C. H., O. C. Okafor, and E. N. Obika. "Design and implementation of a crossflow turbine for Pico hydropower electricity generation." *Heliyon* 6, no. 7 (2020). https://doi.org/10.1016/j.heliyon.2020.e04523
[9] Mehr, Goodarz, Mohammad Durali, Mohammad Hadi Khakrand, and Hadi Hoghooghi. "A novel design and performance optimization methodology for hydraulic Cross-Flow turbines using successive numerical simulations." *Renewable Energy* 169 (2021): 1402-1421. https://doi.org/10.1016/j.renene.2021.01.090
[10] Montanari, Roberto. "Criteria for the economic planning of a low power hydroelectric plant." *Renewable Energy* 28, no. 13 (2003): 2129-2145. https://doi.org/10.1016/S0960-1481(03)00063-6
[11] Picone, Calogero, Marco Sinagra, Luana Gurnari, Tullio Tucciarelli, and Pasquale G. F. Filianoti. "A New Cross-Flow Type Turbine for Ultra-Low Head in Streams and Channels." *Water* 15, no. 5 (2023): 973. https://doi.org/10.3390/w15050973
[12] Sammartano, Vincenzo, Gabriele Morreale, Marco Sinagra, and Tullio Tucciarelli. "Numerical and experimental investigation of a cross-flow water turbine." *Journal of Hydraulic Research* 54, no. 3 (2016): 321-331. https://doi.org/10.1080/00221686.2016.1147500
[13] Siswantara, Ahmad Indra, Budiarso Budiarso, Aji Putro Prakoso, Gun Gun R. Gunadi, Warjito Warjito, and Dendy Adanta. "Assessment of turbulence model for cross-flow pico hydro turbine numerical simulation." *CFD Letters* 10, no. 2 (2018): 38-48.
[14] Mockmore, Charles Arthur, and Fred Merryfield. "The Banki water turbine." *Bulletin series (Oregon State College. Engineering Experiment Station)* (1949).
[15] Desai, Venkappayya R., and Nadim M. Aziz. "An experimental investigation of cross-flow turbine efficiency." *Journal of Fluids Engineering* 116, no. 3 (1994): 545-550. https://doi.org/10.1115/1.2910311
[16] Acharya, Nirmal, Chang-Gu Kim, Bhola Thapa, and Young-Ho Lee. "Numerical analysis and performance enhancement of a cross-flow hydro turbine." *Renewable Energy* 80 (2015): 819-826. https://doi.org/10.1016/j.renene.2015.01.064
[17] Aliman, Isnain, Ika Kurniawati, Josi Ayu Wulandari, and Priyono Sutikno. "Evaluation design and simulation of three-way nozzle and control flow vane nozzle on cross flow water turbine for various head." In *AIP Conference Proceedings*, vol. 1984, no. 1. AIP Publishing, 2018. https://doi.org/10.1063/1.5046631
[18] De Andrade, Jesús, Christian Curiel, Frank Kenyery, Orlando Aguillón, Auristela Vásquez, and Miguel Asuaje. "Numerical investigation of the internal flow in a Banki turbine." *International Journal of Rotating Machinery* 2011 (2011). https://doi.org/10.1155/2011/841214
[19] Sammartano, V., G. Morreale, M. Sinagra, A. Collura, and T. Tucciarelli. "Experimental study of cross-flow micro-turbines for aqueduct energy recovery." *Procedia Engineering* 89 (2014): 540-547. https://doi.org/10.1016/j.proeng.2014.11.476
[20] Sinagra, M., V. Sammartano, C. Aricò, and Alfonso Collura. "Experimental and numerical analysis of a cross-flow turbine." *Journal of Hydraulic Engineering* 142, no. 1 (2016): 04015040. https://doi.org/10.1061/(ASCE)HY.1943-7900.0001061
[21] Sinagra, Marco, Vincenzo Sammartano, Costanza Aricò, Alfonso Collura, and Tullio Tucciarelli. "Cross-Flow turbine design for variable operating conditions." *Procedia Engineering* 70 (2014): 1539-1548. https://doi.org/10.1016/j.proeng.2014.02.170
[22] Adhikari, Ram, and David Wood. "The design of high efficiency crossflow hydro turbines: A review and extension." *Energies* 11, no. 2 (2018): 267. https://doi.org/10.3390/en11020267
[23] Adhikari, R. C., and D. H. Wood. "Computational analysis of part-load flow control for crossflow hydro-turbines." *Energy for Sustainable Development* 45 (2018): 38-45. https://doi.org/10.1016/j.esd.2018.04.003
[24] Adhikari, Ram. "Design improvement of crossflow hydro turbine." *PhD. diss., University of Calgary, Calgary, Canada*, 2016.
[25] Warjito, W., B. Budiarso, K. Celine, and S. B. S. Nasution. "Computational Method for Designing a Nozzle Shape to Improve the Performance of Pico-Hydro Crossflow Turbines." *International Journal of Technology* 12, no. 1 (2021): 139. https://doi.org/10.14716/ijtech.v12i1.4225
[26] Ebhota, Williams S., and Pavel Y. Tabakov. "Design process sequence of crossflow turbine system and the evaluation of structural integrity factors." *International Journal of Energy and Environmental Engineering* 13, no. 3 (2022): 1021-1037. https://doi.org/10.1007/s40095-021-00445-6
[27] Sammartano, Vincenzo, Costanza Aricò, Armando Carravetta, Oreste Fecarotta, and Tullio Tucciarelli. "Banki-Michell optimal design by computational fluid dynamics testing and hydrodynamic analysis." *Energies* 6, no. 5 (2013): 2362-2385. https://doi.org/10.3390/en6052362
[28] Yakhot, Victor, and Steven A. Orszag. "Renormalization-Group Analysis of Turbulence." *Physical Review Letters* 57,

no. 14 (1986): 1722. https://doi.org/10.1103/PhysRevLett.57.1722

[29] Yakhot, Victor, and Steven A. Orszag. "Renormalization group analysis of turbulence. I-Basic theory." *Journal of Scientific Computing* 1, no. 1 (1986): 3-51. https://doi.org/10.1007/BF01061452

[30] Adanta, Dendy, Mochammad Malik Ibrahim, Dewi Puspita Sari, Imam Syofii, and Muhammad Amsal Ade Saputra. "Application of the grid convergency index method and courant number analysis for propeller turbine simulation." *Journal of Advanced Research in Fluid Mechanics and Thermal Sciences* 96, no. 2 (2022): 33-41. https://doi.org/10.37934/arfmts.96.2.3341